

Article

Molecular Hydrogen Microstructures in Planetary Nebulae

Stavros Akras ^{1,2,3,*} , Denise R. Gonçalves ¹, Gerardo Ramos-Larios ⁴  and Isabel Aleman ⁵ 

¹ Observatório do Valongo, Universidade Federal do Rio de Janeiro, 20080-090 Rio de Janeiro, Brazil; denise@astro.ufrj.br

² Instituto de Matemática, Estatística e Física, Universidade Federal do Rio Grande, 96203-900 Rio Grande, Brazil

³ Observatório Nacional/MCTIC, Rua Gen. José Cristino, 77, 20921-400 Rio de Janeiro, Brazil

⁴ Instituto de Astronomía y Meteorología, CUCEI, Guadalajara 44130, Jalisco, Mexico; gerardo.astro@gmail.com

⁵ Instituto de Física e Química, Universidade Federal de Itajubá, Av. BPS 1303, Pinheirinho, 37500-903 Itajubá, Brazil; bebel.aleman@gmail.com

* Correspondence: stavrosakras@gmail.com

Received: 4 March 2020; Accepted: 26 March 2020; Published: 1 April 2020



Abstract: Molecular hydrogen (H₂) emission is commonly detected in planetary nebulae (PNe), specially in objects with bipolar morphologies. New studies showed that H₂ gas is also packed in microstructures embedded in PNe of any morphological type. Despite the presence of H₂ in cometary knots being known for years, only in the last five years, much deeper imagery of PNe have revealed that H₂ also exists in other types of low-ionisation microstructures (LISs). Significant differences are found between the host PNe of cometary knots and other types of LISs, such as nebula age, central star temperature (evolutionary stage) and the absolute sizes of the microstructure itself.

Keywords: astrochemistry; planetary nebulae: NGC 7009, NGC 6543, K 4-47, NGC 7662, Hu 1-2, Hb 12

1. Introduction

Planetary nebulae (PNe) represent the final evolutionary stage of low- and intermediate-mass stars (1–8 M_⊙), and they are formed by the interaction of two or more mass-loss events during the previous stages. The result of these interactions in conjunction with the evolution of the central star (CS) is the development of structures like shells, rims and haloes. Many PNe, however, have been found to possess microstructures (<2–3 arcsec) that are noticeable in low-ionisation emission-lines such as [N II], [S II], and [O I] (e.g., [1,2]). Based on their kinematic characteristics, these microstructures are labeled as: (i) fast low-ionisation emission regions (FLIERS; [2]), (ii) slow moving low ionisation emitting regions (SLOWERS; [3]), and (iii) bipolar, rotating, episodic jets (BRETs; [4]).

A comprehensive review on the morphological and kinematic properties of these microstructures was given by [5], also discussing potential links to various formation models. Interestingly, none of the available formation models are able to sufficiently explain all their properties. Due to their substantial different kinematic properties, all the microstructures were included under one class called *low-ionisation structures* (LISs, [5]). The intriguing enhancement of the low-ionisation emission-lines in these microstructures relative to the surrounding nebular gas has been attributed to either UV radiation from the CS (e.g., [6]) or a combination with shocks (e.g., [7]). Still, little is known about these features.

A particular sub-class of LISs has been found in nearby PNe, namely the cometary knots (CKs) with a long radial tail extended away from the CS [8]. CKs in the Helix, Ring, and Dumbbell nebulae

are known to be composed of molecular hydrogen (H_2) (e.g., [9–12]). Gonçalves and co-workers claimed that LISs should also be dense structures composed of molecular gas, similar to CKs [13]. This could explain their systematic lower electron densities compared to the surrounding nebula values (e.g., [6,7,13]).

In this paper, we present H_2 1-0 S(1) narrow-band images of PNe with low-ionisation structures to discuss the different patterns of the host PNe.

2. Molecular Hydrogen in Microstructures

Besides the presence of H_2 gas in the cometary knots of nearby PNe, new observations over the last five years have unveiled that more LISs are composed of H_2 gas. Fang et al. reported the detection of H_2 emission in microstructures embedded in four PNe. This includes the northwestern knot in Hu 1-2 [14], two pairs of knots in Hb 12 [15], six knots in NGC 7009 [15], and several knots in the halo of NGC 6543 [15] (Figure 1).

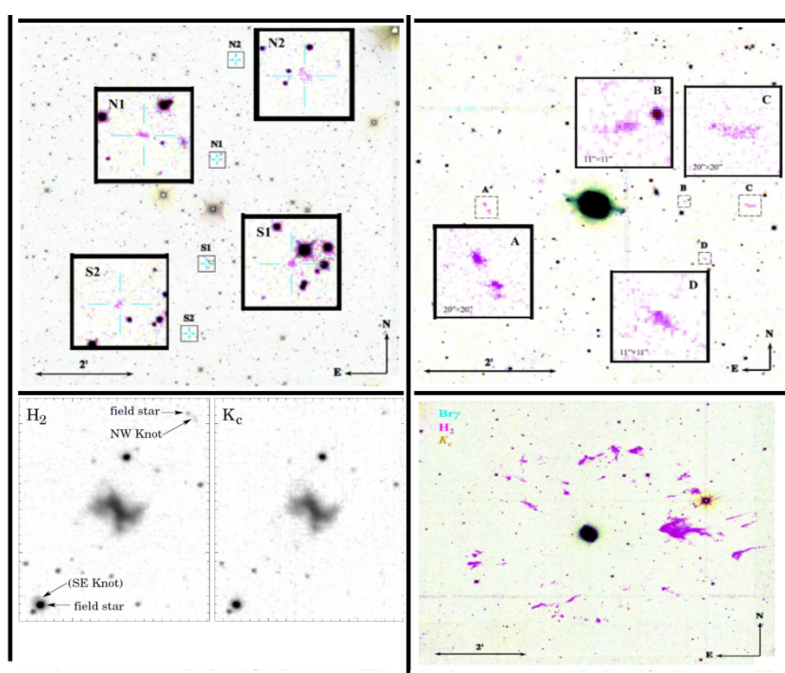


Figure 1. H_2 images of Hb 12 (top-left panel, [14]), NGC 7009 (top-right panel, [15]), Hu 1-2 (bottom-left panel, [15]) and NGC 6543 (bottom-right panel, [15]). The insets on the top panels show a zoom in the H_2 knots.

Deep and high sensitive H_2 imagery of PNe with LISs obtained with the Near InfraRed Imager and Spectrograph (NIRI) at Gemini North have also detected H_2 emission-lines from LISs (K 4-47 and NGC 7662, [16]; NGC 6543 and NGC 7009, [17]) (Figure 2). Note that, the higher spatial resolution of the NIRI images ([17]), revealed H_2 emission from the inner LISs of NGC 6543.

All these H_2 detections associated with LISs (more than 50) have strongly supported the scenario that LISs are composed of molecular gas. A comparison between the CKs and other types of LISs shows a number of differences; so hereafter, we refer to the PNe with CKs as the CKs-PN group and to the PNe with the rest (mostly knots) as the Ks-PN group. Scrutinizing their H_2 images, we find that all knots but those in the elliptical NGC 7662 and in the halo of NGC 6543, lie in the polar direction. This is a perceptible difference between the two groups and it is very likely associated with their formation mechanisms (e.g., thermal instabilities, bullet/jet ejections or AGB fossils).

The two PN groups are characterized by different nebular ages and CS temperatures (T_{eff}) (i.e., evolutionary stages). In particular, the CSs in the CKs-PN group have $T_{eff} > 100$ kK, whilst those in the Ks-PN group cover a wider range, $40 < T_{eff} < 120$ kK (Table 1).

Another pronounced difference between the CKs and knots is that the former are found in younger PNe (≤ 2000 yrs) and the latter in older PNe (> 7000 yrs) for which the CSs have already entered the cooling track (Table 1). The CKs in NGC 6720 are formed after the PN has entered the recombination phase and its CS has entered the cooling track [18]. This mechanism seems not to be applicable for the Ks-PN group, for which the CSs are in earlier evolutionary stage. *What is the link (if any) between CKs and knots? Is the formation mechanism the same?*

It is known that the intensities of H_2 lines around $2 \mu\text{m}$ and $\text{Br}\gamma$ line as well as the $R(H_2)=H_2 1-0 S(1)/H_2 1-2 S(1)$ and $R(\text{Br}\gamma)=H_2 1-0 S(1)/\text{Br}\gamma$ ratios, are strongly dependent on time (evolutionary phase) and the dominant excitation mechanism of H_2 gas [19]. In proto-PN early phase, H_2 excitation is dominated by strong UV radiation. Due to high densities, collisional de-excitation becomes important and results in high $R(H_2)$ ratios (~ 10) and a thermal H_2 emission. For more evolved PNe with $T_{\text{eff}} > 100$ kK (e.g., NGC 6270), H_2 emission has again a thermal origin because of the more important contribution of X-rays. In intermediate phases, the rapid expansion of PNe results in significant decrease of the density and the strength of UV radiation field. Therefore, the excitation of H_2 is again dominated by the UV radiation field, but the de-excitation of gas by collisions is negligible due to the low densities resulting in a $R(H_2)$ ratio close to 3 [20,21].

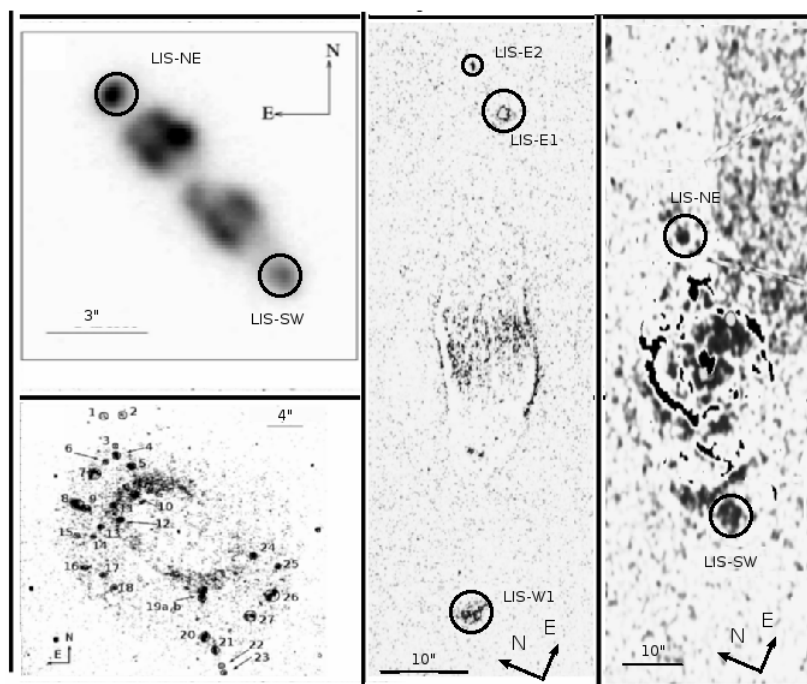


Figure 2. H_2 continuum-subtracted NIRI images of K 4-47 (top-left panel, [16]), NGC 7662 (bottom-left panel, [16]), NGC 7009 (middle panel, [16]) and NGC 6543 (right panel [16]). The circles indicate LIS knots with H_2 emission detected.

The high $R(H_2)$ (~ 10) and $R(\text{Br}\gamma)$ (10–20) values found in the knots of K 4-47 as well as in the CKs of NGC 6270 and NGC 7293 show the two extreme phases (early and late phases in PN evolution), in which H_2 emission has a thermal origin (see Figure 6 in [17]). Shocks cannot be ruled out in the case of the young PN K 4-47, for which high knots' radial velocities ($\sim 100 \text{ km s}^{-1}$) have been measured [22]. The low line ratios (1–2 and 0.1, respectively) measured for the knots in NGC 7662 and NGC 6543 with nebular ages from 1000 to 2000 yrs, indicate UV-fluorescent H_2 emission [17].

NGC 7009 is characterized by low (western knot) and high (eastern knots) $R(H_2)$ values [17]. This implies a different origin for the H_2 emission of each knot. The age of NGC 7009 is similar to those of NGC 7662 and NGC 6543 (Table 1) and its H_2 emission should be dominated by fluorescence. However, the high $R(H_2)$ found in the eastern knots indicates a thermal origin. A density difference between the knots could explain this discrepancy.

Last but not least, the absolute size of the CKs and knots is also different. A rough estimate of the knot's size is given in Table 1, which corresponds to lower values. Knots are at least thrice as big than the CKs. This suggests that the amount of molecular material is likely most relevant in the former.

Table 1. Nebular ages, LISs size, and effective temperatures of central stars.

PN Name	Age [†] (yrs)	T _{eff} ^{††} (kK)	Size ^{†††} (km)	Refs.	PN Name	Age [†] (yrs)	T _{eff} ^{††} (kK)	Size ^{†††} (km)	Refs.
Ks-PN group					CKs-PN group				
PN K 4-47	400–900	120	$>5.2 \times 10^{11}$ ^a	[22]	NGC 6720	7000	110–120	$1-4 \times 10^{10}$	[23,24]
NGC 7662	~1600	100–110	$>1.4 \times 10^{11}$ ^b	[7]	NGC 7293	11,000	110	$1-4 \times 10^{10}$	[24,25]
NGC 6543	1001–1039	65	$>1.7 \times 10^{11}$ ^c	[26]	NGC 6853	>9000	100–110	$1-4 \times 10^{10}$	[24,27]
NGC 7009	1650–2200	80–90	$>1.3 \times 10^{11}$ ^d	[28]					
Hb 12	1357	80–85		[29]					
Hu 1-2	1120	40–50		[30]					

[†] Kinematical age of the nebula, ^{††} Effective temperature of central star, ^{†††} Linear size of LISs; ^a D = 3 kpc [22] and R = 0.585 arcsec [16], ^b D = 1.19 kpc [31] and R ~ 0.4 arcsec [16], ^c D = 1.19/1.5 kpc [32], and R ≥ 0.5 arcsec [17], ^d D = 1.5 kpc [33], and R ≥ 0.3 arcsec [17]. (D ≡ distance and R ≡ radius.)

3. Future Work

Little is known about the formation of LISs in PNe and the excitation mechanisms of their H₂ gas. It is suggested from the above discussion that the host PNe of CKs and other types of LISs are in different evolutionary phases. It is, therefore, necessary to observe a large sample of PNe with LISs, covering different morphological types, CS's temperatures and types of LISs to determine the contribution of UV radiation, shocks and X-ray emission to the excitation of their H₂ gas.

Author Contributions: S.A., methodology; S.A., writing-original draft preparation, conceptualization; D.R.G., G.R.-L., and I.A., validation; S.A., D.R.G., G.R.-L., and I.A., writing-review and editing. All authors have read and agreed to the published version of the manuscript.

Funding: This research was funded by CNPq CAPES, CONACyT and PRODEP.

Acknowledgments: The authors would like to thank the two anonymous referees for the valuable comments and constructive suggestions. IA acknowledges the support of CAPES (Brasil)—Finance Code 001.

Conflicts of Interest: The authors declare no conflict of interest.

References

- Corradi, R.L.M.; Manso, R.; Mampaso, A.; Schwarz, H.E. Unveiling low-ionisation microstructures in planetary nebulae. *Astron. Astrophys.* **1996**, *313*, 913–923.
- Balick, B.; Rugers, M.; Terzian, Y.; Chengalur, J.N. Fast, low-ionisation emission regions and other microstructures in planetary nebulae. *Astrophys. J.* **1993**, *411*, 778–793. [[CrossRef](#)]
- Perinotto, M. Gas Dynamics in Planetary Nebulae: From Macro-structures to FLIERS. *Astrophys. Space Sci.* **2000**, *274*, 205–219. [[CrossRef](#)]
- Lopez, J.A.; Meaburn, J.; Palmer, J.W. Kinematical Evidence for a Rotating, Episodic Jet in the Planetary Nebula Fleming 1. *Astrophys. J. Lett.* **1993**, *415*, L135. [[CrossRef](#)]
- Gonçalves, D.R.; Corradi, R.L.M.; Mampaso, A. Low-ionisation Structures in Planetary Nebulae: Confronting Models with Observations. *Astrophys. J.* **2001**, *547*, 302–310. [[CrossRef](#)]
- Ali, A.; Dopita, M.A. IFU Spectroscopy of Southern Planetary Nebulae V: Low-Ionisation Structures. *Publ. Astron. Soc. Aust.* **2017**, *34*, 36. [[CrossRef](#)]
- Akras, S.; Gonçalves, D.R. Low-ionisation structures in planetary nebulae—I. Physical, kinematic and excitation properties. *Mon. Not. R. Astron. Soc.* **2016**, *455*, 930–961. [[CrossRef](#)]
- O'Dell, C.R.; Balick, B.; Hajian, A.R.; Henney, W.J.; Burkert, A. Knots in Nearby Planetary Nebulae. *Astron. J.* **2002**, *123*, 3329–3347. [[CrossRef](#)]

9. Matsuura, M.; Speck, A.K.; Smith, M.D.; Zijlstra, A.A.; Viti, S.; Lowe, K.T.E.; Redman, M.; Wareing, C.J.; Lagadec, E. VLT/near-infrared integral field spectrometer observations of molecular hydrogen lines in the knots of the planetary nebula NGC 7293 (the Helix Nebula). *Mon. Not. R. Astron. Soc.* **2007**, *382*, 1447–1459. [[CrossRef](#)]
10. Speck, A.K.; Meixner, M.; Jacoby, G.H.; Knezek, P.M. Molecular Hydrogen in the Ring Nebula: Clumpy Photodissociation Regions. *Publ. Astron. Soc. Pac.* **2003**, *115*, 170–177 [[CrossRef](#)]
11. Baldrige, S.P. Small-Scale Structures in Planetary Nebulae. Ph.D. Thesis, University of Missouri, Columbia, MO, USA, 2017.
12. Huggins, P.J.; Forveille, T.; Bachiller, R.; Cox, P.; Ageorges, N.; Walsh, J.R. High-Resolution CO and H₂ Molecular Line Imaging of a Cometary Globule in the Helix Nebula. *Astrophys. J. Lett.* **2002**, *573*, L55. [[CrossRef](#)]
13. Gonçalves, D.R.; Mampaso, A.; Corradi, R.L.M.; Quireza, C. Low-ionisation pairs of knots in planetary nebulae: Physical properties and excitation. *Mon. Not. R. Astron. Soc.* **2009**, *398*, 2166–2176. [[CrossRef](#)]
14. Fang, X.; Guerrero, M.A.; Miranda, L.F.; Riera, A.; Velázquez, P.F.; Raga, A.C. Hu 1-2: A metal-poor bipolar planetary nebula with fast collimated outflows. *Mon. Not. R. Astron. Soc.* **2015**, *452*, 2445–2462. [[CrossRef](#)]
15. Fang, X.; Zhang, Y.; Kwok, S.; Hsia, C.-H.; Chau, W.; Ramos-Larios, G.; Guerrero, M.A. Extended Structures of Planetary Nebulae Detected in H₂ Emission. *Astrophys. J.* **2018**, *859*, 92. [[CrossRef](#)]
16. Akras, S.; Gonçalves, D.R.; Ramos-Larios, G. H₂ in low-ionisation structures of planetary nebulae. *Mon. Not. R. Astron. Soc.* **2017**, *465*, 1289–1296. [[CrossRef](#)]
17. Akras, S.; Gonçalves, D.R.; Ramos-Larios, G.; Isabel, A. H₂ Emission in the Low-ionisation Structures of the Planetary Nebulae NGC 7009 and NGC 6543. *Mon. Not. R. Astron. Soc.* **2020**, to be published. [[CrossRef](#)]
18. van Hoof, P.A.M.; van de Steene, G.C.; Barlow, M.J.; Exter, K.M.; Sibthorpe, B.; Ueta, T.; Peris, V.; Groenewegen, M.A.T.; Blommaert, J.A.D.L.; Cohen, M.; et al. Herschel images of NGC 6720: H₂ formation on dust grains. *Astron. Astrophys.* **2010**, *518*, 137–144. [[CrossRef](#)]
19. Natta, A.; Hollenbach, D. The evolution of the neutral gas in planetary nebulae: Theoretical models. *Astron. Astrophys.* **1998**, *337*, 517–538.
20. Sternberg, A.; Dalgarno, A. The infrared response of molecular hydrogen gas to ultraviolet radiation - High-density regions. *Astrophys. J.* **1989**, *338*, 197–233. [[CrossRef](#)]
21. Burton, M.G.; Hollenbach, D.J.; Tielens, A.G.G.M. Line emission from clumpy photodissociation regions. *Astrophys. J.* **1990**, *365*, 620–639. [[CrossRef](#)]
22. Corradi, R.L.M.; Gonçalves, D.R.; Villaver, E.; Mampaso, A.; Perinotto, M.; Schwarz, H.E.; Zanin, C. High-Velocity Collimated Outflows in Planetary Nebulae: NGC 6337, HE 2-186, and K 4-47. *Astrophys. J.* **2000**, *535*, 823–832. [[CrossRef](#)]
23. O’Dell, C.R.; Sabbadin, F.; Henney, W.J. The Three-Dimensional ionisation Structure and Evolution of NGC 6720, The Ring Nebula. *Astron. J.* **2007**, *134*, 1679–1692. [[CrossRef](#)]
24. O’Dell, C.R.; Balick, B.; Hajian, A.R.; Henney, W.J.; Burkert, A. Knots in Planetary Nebulae. *Rev. Mex. Astron. Astrofis.* **2003**, *15*, 29–33.
25. Meaburn, J.; López, J.A.; Richer, M.G. Optical line profiles of the Helix planetary nebula (NGC 7293) to large radii. *Mon. Not. R. Astron. Soc.* **2008**, *384*, 497–503. [[CrossRef](#)]
26. Reed, D.S.; Balick, B.; Hajian, A.R.; Klayton, T.L.; Giovanardi, S.; Casertano, S.; Panagia, N.; Terzian, Y. Hubble Space Telescope Measurements of the Expansion of NGC 6543: Parallax Distance and Nebular Evolution. *Astron. J.* **1999**, *118*, 2430–2441. [[CrossRef](#)]
27. Meaburn, J.; Boumis, P.; Christopoulou, P.E.; Goudis, C.D.; Bryce, M.; López, J. A. The Global Kinematics of the Dumbbell Planetary Nebula (NGC 6853, M27, PN G060.8-03.6). *Rev. Mex. Astron. Astrofis.* **2005**, *41*, 109.
28. Sabbadin, F.; Turatto, M.; Cappellaro, E.; Benetti, S.; Ragazzoni, R. The 3-D ionisation structure and evolution of NGC 7009 (Saturn Nebula). *Astron. Astrophys.* **2004**, *416*, 955–981. [[CrossRef](#)]
29. Vaytet, N.M.H.; Rushton, A.P.; Lloyd, M.; López, J.A.; Meaburn, J.; O’Brien, T.J.; Mitchell, D.L.; Pollacco, D. High-speed knots in the hourglass-shaped planetary nebula Hubble 12. *Mon. Not. R. Astron. Soc.* **2009**, *398*, 385–393. [[CrossRef](#)]
30. Miranda, L.F.; Blanco, M.; Guerrero, M.A.; Riera, A. The collimated outflows of the planetary nebula Hu 1-2: Proper motion and radial velocity measurements. *Mon. Not. R. Astron. Soc.* **2012**, *421*, 1661–1665. [[CrossRef](#)]
31. Mellema, G. On expansion parallax distances for planetary nebulae. *Astron. Astrophys.* **2004**, *416*, 623–629. [[CrossRef](#)]

32. Gómez-Gordillo, S.; Akras, S.; Gonçalves, D.R.; Steffen, W. Distance mapping applied to four well-known planetary nebulae and a nova shell. *Mon. Not. R. Astron. Soc.* **2020**, *492*, 4097–4111. [[CrossRef](#)]
33. Schönberner, D.; Steffen, M. Confronting expansion distances of planetary nebulae with Gaia DR2 measurements. *Astron. Astrophys.* **2019**, *625*, 137–144. [[CrossRef](#)]



© 2020 by the authors. Licensee MDPI, Basel, Switzerland. This article is an open access article distributed under the terms and conditions of the Creative Commons Attribution (CC BY) license (<http://creativecommons.org/licenses/by/4.0/>).